Contrib Mineral Petrol (1988) 98:64–71

Contributions to Mineralogy and Petrology

Sapphirine and spinel phase relationships in the system $FeO-MgO-Al_2O_3-SiO_2-TiO_2-O_2$ in the presence of quartz and hypersthene

Roger Powell and Michael Sandiford
Department of Geology, University of Melbourne, Parkville, Victoria 3052, Australia

Abstract. Sapphirine and spinel can accommodate significant ferric iron and therefore the mineral equilibria involving these phases must be sensitive to $a(O_2)$. In this paper we examine the theoretical phase relationships involving sapphirine and spinel in addition to sillimanite, garnet, cordierite, rutile, hematite-ilmenite solid solution (henceforth ilmenite), and magnetite-ulvospinel solid solution (henceforth magnetite), in the presence of quartz and hypersthene in the system $FeO-MgO-Al_2O_3-SiO_2-TiO_2-O_2$ (FMASTO), with particular reference to the topological inversion in P–T postulated by Hensen (Hensen 1986). Documented natural associations suggest that the appropriate topology for assemblages involving magnetite and ilmenite is Hensen's higher $a(O_2)$ one, while, in contrast, the topology for assemblages involving ilmenite and rutile is the lower $a(O_2)$ one. The exact configuration of the inversion between these two topologies remains uncertain because of uncertainties in the ferric/ferrous iron partitioning between sapphirine and spinel-cordierite at high temperatures. By comparison with experimental data and natural occurences, the sillimanite-sapphirine-cordierite-garnet-hypersthene-quartz assemblage is in equilibrium at about 1000°–1020° C and 7–8 kbars, while sapphirine-cordierite-spinel-garnet-hypersthene-quartz occurs at temperatures in excess of those attainable during crustal metamorphism, for ilmenite-rutile buffered assemblages. This implies that sapphirine-rutile-hypersthene-quartz assemblages, as found in the Napier Complex, Antarctica, can only occur at >1000° C. Also, spinel-rutile-hypersthene-quartz assemblages should not be found in rocks because temperatures in excess of 1100° C are expected to be involved in their formation. The temperatures of formation of spinel-sillimanite-sapphirine-garnet-hypersthene-quartz, sapphirine-spinel-cordierite-sillimanite-hypersthene-quartz, and sillimanite-spinel-cordierite-garnet-hypersthene-quartz in assemblages buffered by magnetite and ilmenite are less well constrained, but are likely to be in the range 900°–1000° C. These conclusions apply to rocks with compositions close to FMASTO; the perturbing effects of substantial concentrations of additional components, in particular Ca, mainly in garnet, and Zn and Cr, mainly in spinel, may invalidate these conclusions.

Introduction

Mineral assemblages involving sapphirine and/or spinel with quartz have been the focus of several studies recently, and the subject of some controversy. The attraction of these rocks is that they formed at more or less extreme conditions of metamorphism (e.g., Hensen and Green 1973; Sandiford and Powell 1986), and as one consequence, usually show spectacular corona textures reflecting post-metamorphic reequilibration. The mineralogical relationships in these coronas enable the determination of pressure-temperature vectors for the cooling of these high grade terrains if the phase relationships in appropriate systems are known, and if the effects of pressure and temperature can be isolated from other effects. Of course, pressure-temperature vectors are critical data in understanding the tectonothermal evolution of orogenic belts.

Controversy surrounds the phase relationships in systems appropriate to these rocks. The detailed experimental study of Hensen in the early 1970's (summarized in Hensen and Green 1973) on a model pelite system, $FeO-MgO-Al_2O_3-SiO_2$, at $a(O_2)$ more reducing than QFM, provides an explanation of many of the observed phase relationships in rocks at highest grade which are in or close to this system. The topology of the reactions is shown in Fig. 1a. However there are rocks, apparently formed under more oxidized conditions, with relationships inconsistent with the topology of Fig. 1a, for example the development of sillimanite coronas between cordierite and spinel in the presence of hypersthene and quartz in the Labwor Hills rocks (Sandiford et al. 1987). In response to the recognition of these inconsistencies, some authors reject Hensen's work and derive alternative topologies for the system (e.g., Vielzeuf 1983). An additional reason why these authors dismiss Hensen's work has been that workers have found the very high temperatures (>1000° C) indicated by Hensen's phase relationships unpalatable.

Hensen has shown more recently (Hensen 1986) that a logical way of accounting for the inconsistencies between some observed phase relationships and his own experimental results is to consider how the phase relationships might change with increasing oxygen activity. Hensen argued that the main effect of increasing oxygen activity is to stabilize spinel-bearing assemblages with respect to other assemblages, and this ultimately leads to an inversion of topology, Fig. 1a to b, with invariant points [spinel] and [sillimanite] stable at low oxygen activity, and [sapphirine], [garnet] and [cordierite] stable at high oxygen activity. Clearly, in order to extract the maximum information concerning the *P–T* history of sapphirine-spinel-quartz rocks, it is necessary to understand the total assemblage, including both silicate and oxide phases. This paper concerns the extension of Hensen's logic into the system $FeO-MgO-Al_2O_3-SiO_2-TiO_2-$

Offprint requests to: R. Powell

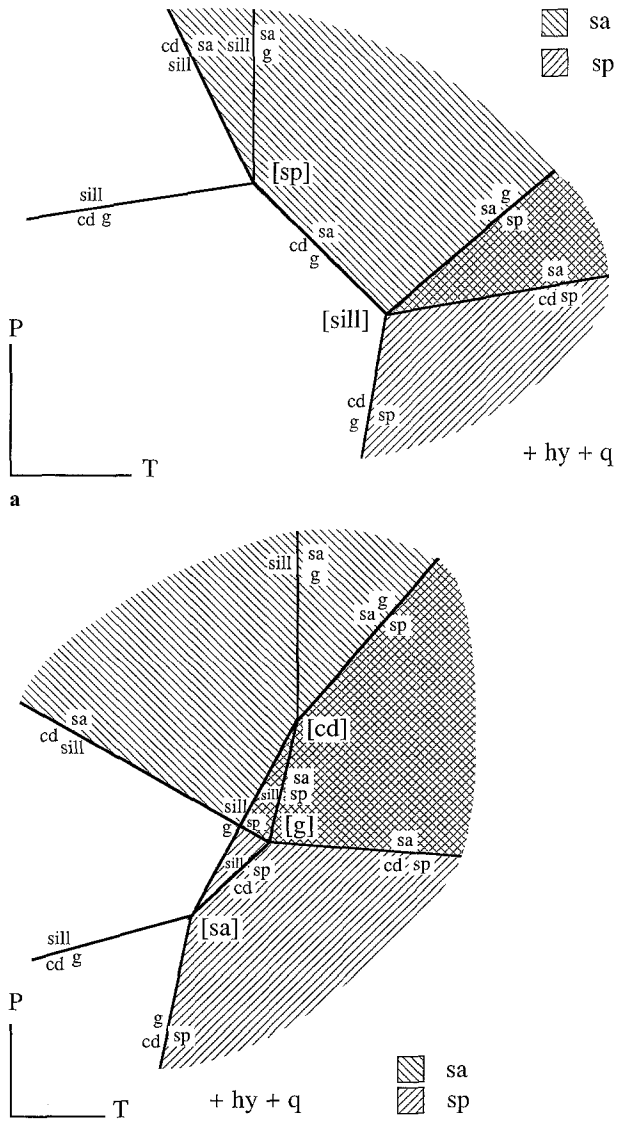

Fig. 1 a, b. Pressure-temperature diagrams at (**a**) a fixed low oxygen activity, and (**b**) a fixed high oxygen activity (after Hensen 1986, Fig. 1). The diagrams are for quartz- and hypersthene-saturated systems. Note that in **a**, [spinel] and [sillimanite] are stable, and [sapphirine], [garnet] and [cordierite] are metastable, whilst in **b**, [sapphirine], [garnet] and [cordierite] are stable and [spinel] and [sillimanite] are metastable. This simple antipathetic relationship implies that **a** and **b** are related by a simple inversion of topology, due most obviously to an increase of oxygen activity (Hensen 1986, Fig. 2). Note that the only reactions which are exclusive to each topology are those connecting the invariant points. The *abbreviations* used here and in later diagrams are: *g* garnet, *cd* cordierite, *sp* spinel, *sa* sapphirine, *sill* sillimanite, *hy* hypersthene and *q* quartz

O_2 (FMASTO), so that the Fe–Ti oxides coexisting with the silicate assemblages can be considered explicitly.

Phase relationships

The first requirement is to derive a diagram on which compatibility relationships can be shown. FMASTO must be reduced by at least two dimensions to achieve this on a 2-D piece of paper. The first obvious restriction is to confine attention to quartz-saturated systems, although this means that only those sapphirine- and/or spinel-bearing assemblages in the highest grade terrains can be considered.

$FeO-MgO-Al_2O_3-SiO_2-O_2+quartz$

Ignoring TiO_2 temporarily, compatibility relationships in the quartz-saturated FMASO system can be shown in a tetrahedron, Fig. 2a. There is some consensus that the order of $Mg/(Mg+Fe^{2+})$ is cordierite > sapphirine > hypersthene > spinel > garnet (e.g., Hensen 1986). These relationships are reflected in the relative positions of the phases with respect to planes containing O_2 and Al_2O_3 in Fig. 2a. Much less is known about the relative oxidation of these silicates, say in terms of $Fe^{3+}/(Mg+Fe^{2+})$, as reflected in the relative positions of the phases with respect to planes containing Al_2O_3 and MgO in Fig. 2a. Hensen considers that spinel is likely to be the most oxidized mineral, but points out that exsolution of magnetite during cooling leaves a spinel with relatively low Fe^{3+}. Our experience is similar to this; in the Labwor Hills rocks for example, spinel has low Fe^{3+}, but has abundant magnetite exsolution lamellae, whilst sapphirine has relatively high Fe^{3+}, but is relatively poor in exsolved oxide species (Sandiford et al. 1987). Given the problems introduced by continued equilibration of spinel and possibly sapphirine during cooling, we cannot determine the order of oxidation of spinel and sapphirine from rocks. In the following we consider the possibility that either phase may be the more oxidized at high temperature.

Of the remaining minerals, hypersthene is likely to be the more oxidized, and cordierite and garnet the least oxidized. The compatibility relationships shown in Fig. 2a, for relatively high T moderate P conditions outside the sapphirine stability field, reflect the oxidation relationships discussed above. The range of compositions for spinel are confined to the plane containing $Fe_3O_4-FeAl_2O_4-MgAl_2O_4$. The range of compositions for garnet and cordierite are essentially contained in the plane, $FeO-MgO-Al_2O_3$. Hypersthene shows a range of composition towards Al_2O_3 and into the tetrahedron as a consequence of various Tschermak's substitutions. The position of the tie tetrahedron involving spinel-cordierite-garnet-hypersthene indicates that for bulk compositions near the $FeO-MgO-Al_2O_3$ plane at low oxygen activities, the garnet-cordierite tie line is stable, whereas for bulk compositions well into the tetrahedron at higher oxygen activities, the spinel-hypersthene tie line is stable. In other words, spinel-bearing assemblages are stabilized by increased oxygen activity.

$FeO-MgO-Al_2O_3-SiO_2-O_2$ + quartz + hypersthene

Returning to the reduction of dimension of the compatibility diagram, we have chosen to project from hypersthene in addition to quartz because it is normally present in quartz-bearing assemblages in this system at high grade. As emphasized by Thompson (1979), there is no particular difficulty projecting from a variable composition phase, in this case hypersthene, as long as it is recognized that the projected phase relationships are in equilibrium with hypersthenes of different compositions, and as long as the projection plane lies between the projecting phase and all (variable composition) phases to be projected. The chosen projection plane is $Fe_3O_4-Mg_3O_4-Al_4O_4$, which includes garnet

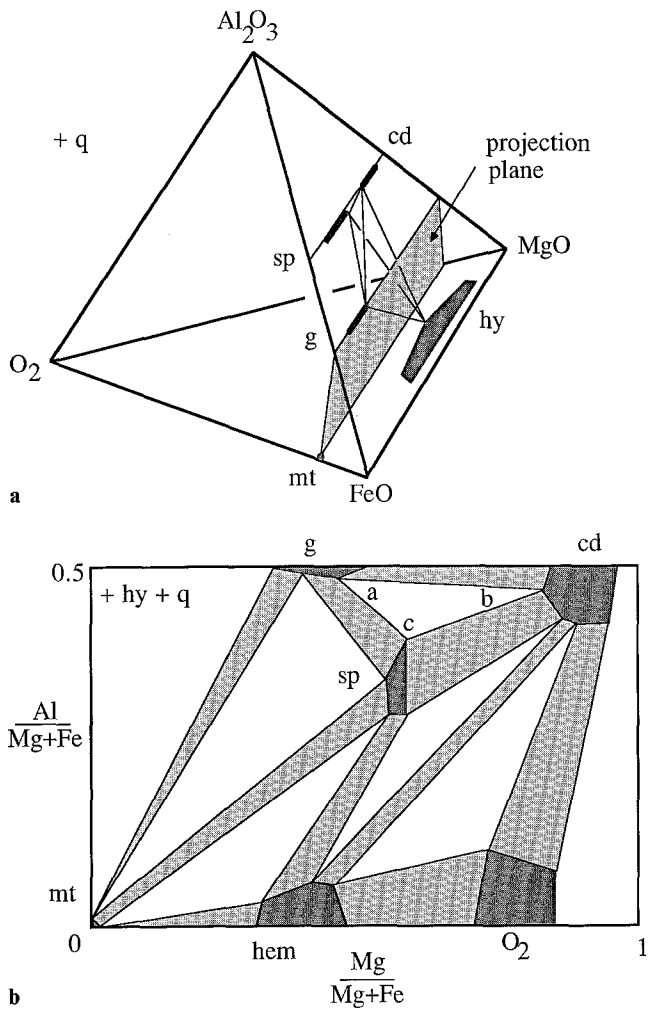

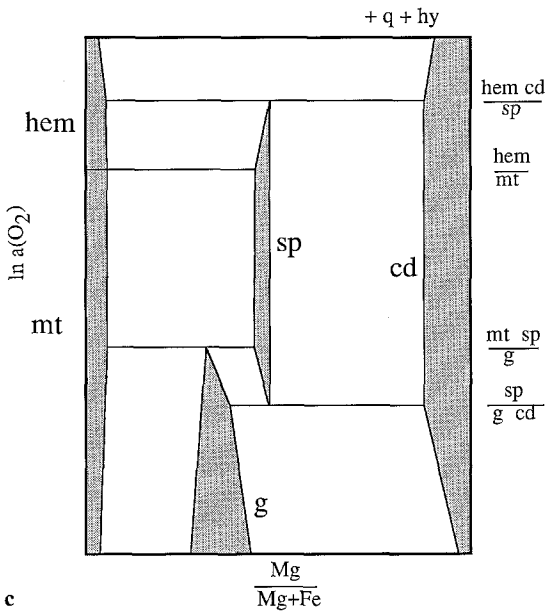

Fig. 2a–c. **a** A qualitative $FeO-MgO-Al_2O_3-O_2$ compatibility diagram, projected from quartz, for a relatively high temperature inside the stability field of garnet + cordierite. The plane onto which phase relationships are to be projected from hypersthene is *shaded*. Note that the tie tetrahedron hypersthene-garnet-cordierite-spinel intersects this projection plane to form a *tie triangle*, marked as *a-b-c* in **b**. **b** A compatibility diagram, corresponding to **a**, drawn orthogonally, involving projection from hypersthene and quartz. Additional relationships involving magnetite, hematite and O_2 are also included. Note the transcription of the tie tetrahedron from **a** to the *tie triange*, *a–b–c*, in **b** (see text for further discussion). Additional *abbreviations* are *mt* magnetite and *hem* hematite. **c** A ln $a(O_2)$-x diagram corresponding to **b**, treating O_2 as an intensive variable, rather than as an apex of a compatibility diagram as in **a**. In **b**, **c**, Fe in the axis annotations is Fe^{2+}

compositions in this system. Where the tie tetrahedron in Fig. 2a penetrates the projection plane is the projection of the tie tetrahedron onto this plane. The projection plane drawn orthogonally, and showing the resulting tie triangle, a–b–c, are shown on Fig. 2b, along with plausible compatibility relationships involving magnetite, hematite and O_2. Note that the one phase fields for hematite and oxygen are extensive, even though they plot as points in Fig. 2a. This is because there is a bundle of tie lines between each of these phases and hypersthenes of different compositions.

Figure 2b can be contoured for oxygen activity, with contours coinciding with tie lines in two phase fields, and oxygen activity being fixed in three phase fields, the assemblage buffering oxygen activity. Adding oxygen activity as a third dimension to Fig. 2b, with oxygen activity increasing out of the page, the diagram becomes like a "cascade" descending away from the O_2 field, with one and two phase fields being "waterfalls" and three phase fields being "pools". A horizontal section of this diagram at constant oxygen activity will in general only see one or two phase fields. In fact the three phase fields in Fig. 2b correspond to reactions in the system considered as binary with oxygen activity as a variable.

The connection now needs to be made between the more or less familiar diagrams of Fig. 1 and diagrams like Fig. 2c. The first thing to note is that the *PT* diagrams of Fig. 1 are at fixed oxygen activity so they correspond to horizontal sections at the required oxygen activity of diagrams like Fig. 2c for the range of temperatures and pressures involved. A consequence of this is that diagrams like Fig. 1 are not particularly useful unless the system being considered is buffered for oxygen, thus having fixed oxygen activity. If the $a(O_2)$ in the system is not fixed, then diagrams like Fig. 1 are inappropriate because the reactions move in pressure-temperature-oxygen activity space.

In order to clarify the meaning of the diagrams in Fig. 1, oxygen must be included in the reactions shown. Of course there will be a diagram, in fact with the topology of Fig. 1a, (Hensen 1986; Harley 1986) for very low oxygen activity in which the minerals are essentially Fe^{3+}-free, so reactions between the minerals involve negligible O_2. However, for finite oxygen activities, the partitioning of Fe^{3+} between the minerals will lead to oxygen being involved in all the reactions depicted in Fig. 1. Focussing on reactions around the [sillimanite] invariant point, Fig. 3a is a compatibility diagram showing the positions of the phases using agreed relative $Mg/(Mg+Fe^{2+})$ values and using the relative oxidation states discussed earlier. We will now show the effect of different sapphirine compositions, given an appropriate spinel composition, on the direction [sillimanite] moves as oxygen activity is changed. Considering first $sapphirine_1$, with the composition sa_1 in Fig. 3a, O_2 can be placed on

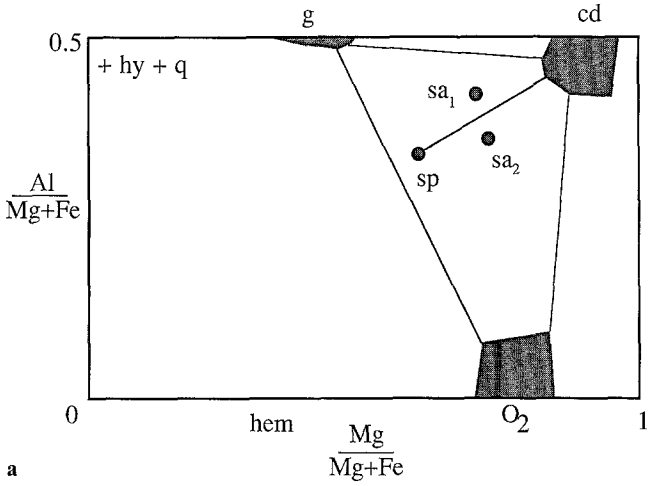

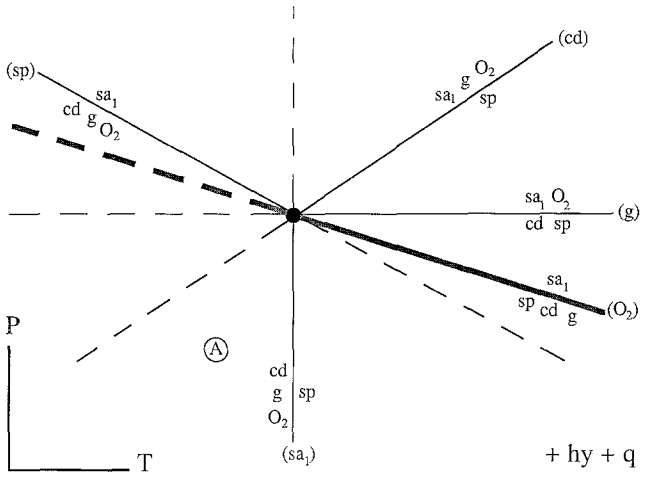

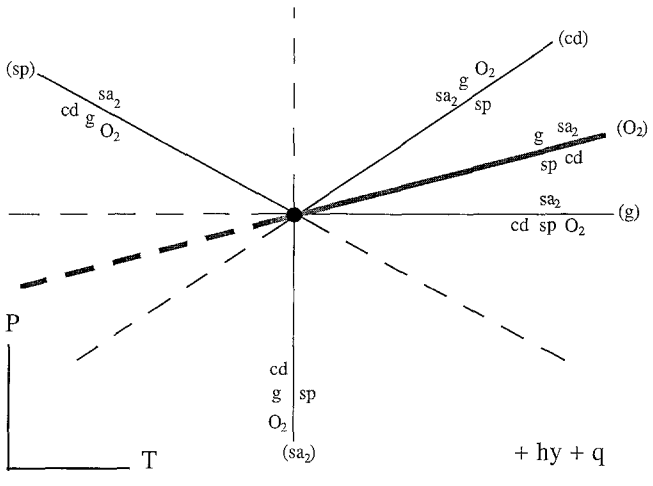

Fig. 3a–c. a A compatibility diagram for the system FMASO projected from hypersthene and quartz, illustrating the alternative relative positions of sapphirine with respect to *tie-lines* between cordierite and spinel. **b, c** *P–T* diagrams for [sillimanite] for the alternative compositions of sapphirine, sa_1 and sa_2, respectively. Note the change in position of (O_2), and the position of O_2 in (garnet), between **b** and **c**. Point *A* in **b** is referred to in the text

the appropriate sides of the reactions in Fig. 1a using the relative positions of the phases in Fig. 3a, giving Fig. 3b. Having done this, it is clear where an (O_2) reaction must be placed using Schreinemakers Rule, Fig. 3b (thicker line).

The relationship between Fig. 3b and Fig. 2a can now be established. Consider that the low oxygen activity *PT* grid in Fig. 3b is actually at sufficiently low $a(O_2)$ that the minerals are effectively Fe^{3+}-free, then for the *PT* of point A, this grid gives the phase relations near the $FeO-MgO-Al_2O_3$ face of Fig. 2a, with the garnet-cordierite tie line stable. As oxygen activity increases, [sillimanite] tracks along its (O_2) reaction, and at some oxygen activity, the reaction:

garnet + cordierite = spinel + hypersthene

passes through A. The point of passage corresponds to the tie tetrahedron in Fig. 2a. At higher oxygen activities, A is now on the high temperature side of the reaction, and the spinel-hypersthene tie line is stable, corresponding to compositions well within the tetrahedron in Fig. 2a. This line of logic is important because it shows how diagrams like Fig. 4 give information on the way the mineral assemblage of a particular bulk composition (excluding oxygen) depends on oxygen activity.

The (O_2) reaction on Fig. 3b has no clear relevance if Fig. 3b is viewed as a *PT* diagram at arbitrary fixed oxygen activity, for example, for an externally buffered system. However (O_2) is obviously a significant line because it is along this line that [sillimanite] moves as oxygen activity changes, so, combined with where the (O_2) reactions are for the other invariant points, it controls whether and where an inversion of topology occurs (Hensen 1986; Sandiford et al. 1987). An inversion of topology, from the relationships in Fig. 1a to those in Fig. 1b, occurs to higher oxygen activity if the metastable extensions of the (O_2) reactions from stable invariant points intersect, implying that, at some oxygen activity, all the invariant points superpose. If the inversion is to occur to lower oxygen activity then the stable parts of the (O_2) reactions must intersect.

For the spinel and sapphirine compositions suggested in Fig. 3a, there are two possibilities for the position of the metastable extension of (O_2): the first, with $sapphirine_1$ is the one drawn in Fig. 3b; the second, with $sapphirine_2$, involves (O_2) lying between (garnet) and (cordierite). For this second choice, as shown in Fig. 3c, the only labelling change to accomodate $sapphirine_2$ in Fig. 3b is for O_2 to change sides on (garnet), and for the (O_2) reaction to become:

garnet + sapphirine = spinel + cordierite

Other positions for (O_2) are excluded because they require spinel and/or sapphirine to be less oxidized than hypersthene and therefore to plot above the garnet-cordierite tie line in Fig. 3a.

If it is assumed that the position of sapphirine relative to the spinel-cordierite tie-line is maintained over the pressure-temperature range of interest, then Fig. 4 illustrates the two ways in which an inversion of topology can occur. Fig. 4a is for sapphirine above spinel-cordierite in Fig. 3a, e.g., for $sapphirine_1$, whereas Fig. 4b is for sapphirine below spinel-cordierite in Fig. 3a, e.g., for $sapphirine_2$. Given that magnetite exsolution from spinel occurs during cooling, thus changing the spinel composition, then a combination of Fig. 4a and b is possible if the spinel composition

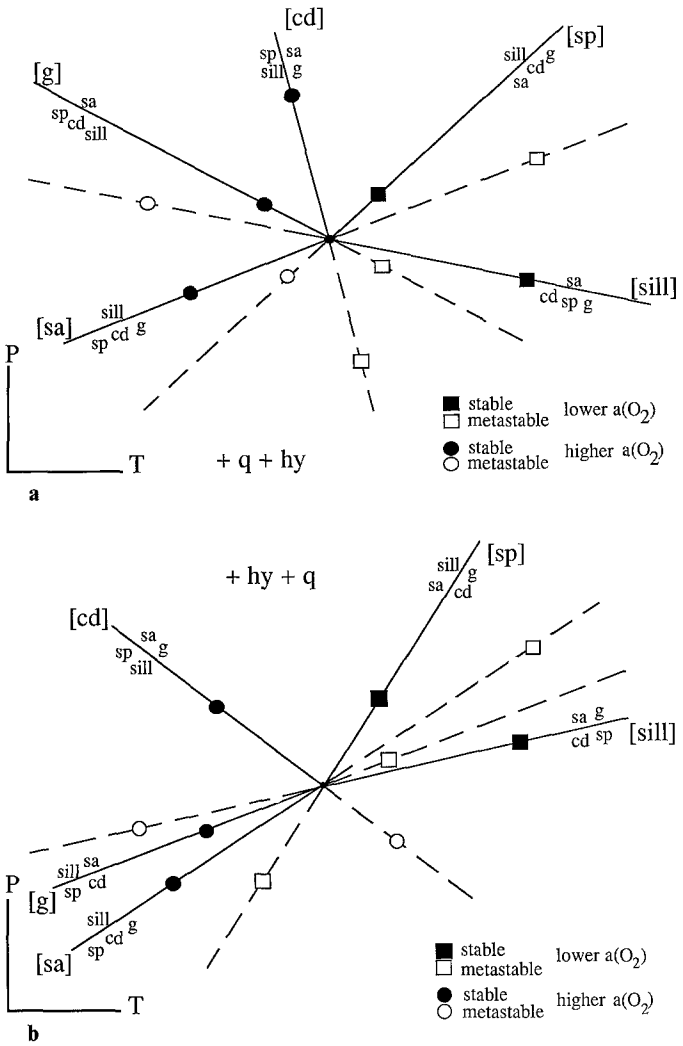

Fig. 4a, b. P–T diagrams showing the position of all (O_2) reactions (*heavy lines*) for **a** sa_1, and **b** sa_2. The (O_2) reactions are the *lines* along which the intersections in the fixed $a(O_2)$ grids move as $a(O_2)$ is changed. The *squares* and *circles* correspond to the positions of the intersections in Fig. 1 for examples of high and low constant $a(O_2)$. *Closed symbols* are stable intersections, *open* are metastable

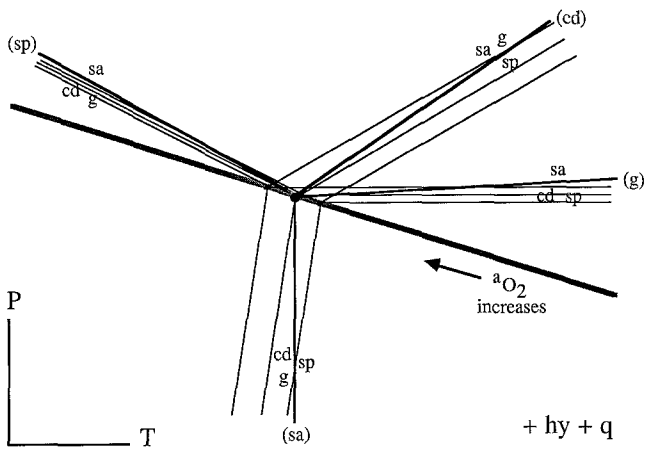

Fig. 5. *P–T* diagram for [sillimanite] illustrating the relationship between the positions of reactions for constant $a(O_2)$ conditions, *light lines*, and mineral buffered $a(O_2)$ conditions, *heavy lines*. As $a(O_2)$ increases, the intersection slides along the thick *patterned line* to lower temperature

moves through collinearity with sapphirine and cordierite in the temperature range of Fig. 4. In that case the higher temperature relationships might be those of Fig. 4a, the lower temperature relationships those of Fig. 4b.

Understanding Fig. 4 for buffered situations requires care. As already emphasised, the diagrams in Fig. 1 are for fixed values of $a(O_2)$. In systems buffered by mineral equilibria, oxygen activity is a function of temperature and, to a lesser extent, pressure, according to the equilibria involved. A consequence of this is that a grid like Fig. 3b is slightly transformed if the grid is to apply to such a buffered situation, Fig. 5. There should be no topological consequences of treating diagrams like Fig. 1 as applying to buffered systems, rather than constant $a(O_2)$ ones, because the temperature dependence of most mineral equilibria buffers is small, and the pressure dependence unimportant, for the temperature and pressure range of interest. This logic is appropriate for considering external buffering, as in the capsule-in-capsule experimental technique used to buffer $a(O_2)$, or if the phases involved in the buffer are in the system but do not involve components which form solid solutions with the minerals of interest, apart from O_2. This caveat is required if, for example, we consider FMASO buffered by magnetite and hematite, with these phases being an integral part of the mineral assemblage. In this case considering Fig. 5, it is clear that this diagram is not appropriate to magnetite-hematite bearing assemblages as the system depicted would then have a variance of -1. Of course this is a consequence of magnetite and hematite being phases in FMASO. In nature, this problem does not occur as significant TiO_2 is usually found in the oxide phases.

$FeO-MgO-Al_2O_3-SiO_2-TiO_2-O_2$ + hypersthene + quartz

Addition of TiO_2 to the system already considered allows buffers in the system, particularly magnetite-ilmenite and rutile-ilmenite, to be part of the mineral assemblage, and for diagrams like Fig. 5 to be appropriate. (Magnetite is used in the sense of magnetite-ulvospinel solid solutions, ilmenite in the sense of hematite-ilmenite solid solutions.) Looking at the reaction (garnet) in Fig. 5, this reaction becomes:

sapphirine + ilmenite = cordierite + spinel + rutile

and is depicted in Fig. 6. Note that ilmenite and rutile must swap sides in this reaction if the other sapphirine composition is appropriate. A *P–T* grid for FMASTO, incorporating petrological constraints, is presented in the next section.

Discussion

Sapphirine-quartz and spinel-quartz assemblages containing magnetite and/or ilmenite have been documented from a number of localities (Morse and Talley 1971; Nixon et al. 1973; Caporuscio and Morse 1978; Vielzeuf 1983; Sandiford et al. 1987). In contrast, sapphirine-quartz-rutile assemblages are comparatively rare, being known principally from Enderby Land, Antarctica (Ellis et al. 1980; Harley

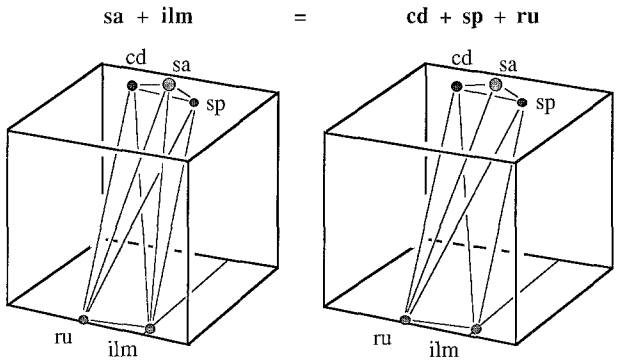

Fig. 6. Orthogonal compatibility diagrams in FMASTO projected from hypersthene and quartz, illustrating the reaction sapphirine + ilmenite = cordierite + spinel + rutile. Additional *abbreviations* are *ru* rutile and *ilm* ilmenite

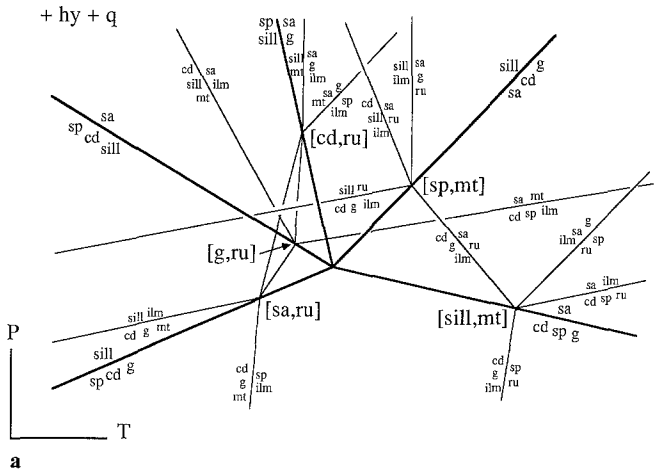

a

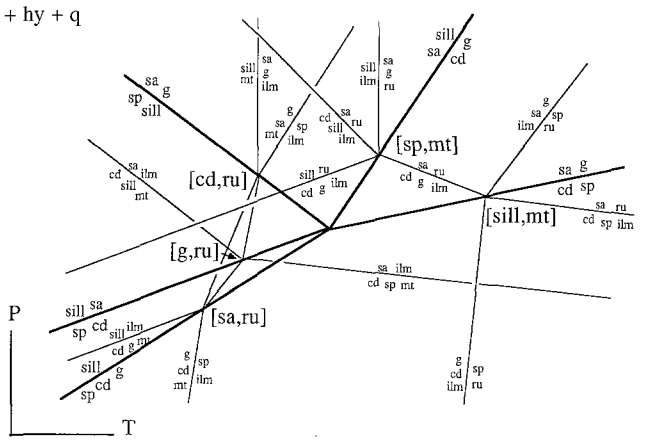

b

Fig. 7a, b. *P–T* grids for FMASTO projected from hypersthene and quartz for **a**, sa_1, and **b**, sa_2. **a** and **b** correspond broadly to Fig. 4a and b. In general, $a(O_2)$ in the reactions increases from higher temperature to lower temperature, from (*mt*) to (*ru*) reactions

1985, 1986; Sandiford 1985), but also from the Gruf Complex (Droop and Bucher-Nurminen 1984). We know of no documented occurrences of spinel-rutile-hypersthene-quartz assemblages where the spinel is restricted to the system, FMASTO.

As shown by Hensen (1986) and more recently by Sandiford et al. (1987) the magnetite-ilmenite buffered assemblages are accounted for by the "inverted" topology involving stable [garnet], [cordierite] and [sapphirine] invariant points. In particular, the occurrence of sillimanite-spinel-hypersthene-quartz-magnetite-ilmenite associations from the Labwor Hills provides critical evidence for the validity of this topology at high $a(O_2)$. In contrast, the Enderby Land and Gruf Complex assemblages, in which $a(O_2)$ was controlled by, or lower than, the ilmenite-rutile buffer, appear to be accounted for by the "normal" topology involving stable [sillimanite] and [spinel] (Hensen 1986; Harley 1986). As a consequence of these observations, a *P–T* petrogenetic grid can be drawn for the system, FMASTO, with the topological inversion located in a region of *P–T*-$a(O_2)$ space accessible to pelitic rock compositions in the crust.

The remaining problem concerning the inversion relates to the state of oxidation of sapphirine relative to the spinel-cordierite tie line, Fig. 3a. We might expect to be able to discriminate between the alternative topologies shown in Fig. 7 on the basis of reaction textures in rocks, but unfortunately we know of no textures which unequivocally do this. For instance, in the Labwor Hills rocks retrograde sapphirine forms coronas on, and appears to grow at the expense of prograde ilmenite, magnetite and spinel (in the presence of cordierite, hypersthene and quartz), whereas in Fig. 7a and b the responsible reactions might be:

for sa_1: cordierite + spinel + ilmenite = sapphirine + magnetite

and:

for sa_2 cordierite + spinel + magnetite = sapphirine + ilmenite

respectively. The apparent lack of diagnostic reaction textures in this case may reflect that a collinearity is developed between sapphirine, cordierite and spinel (with excess hypersthene and quartz) due to changing oxidation state of spinel and/or sapphirine during cooling, in the temperature range of interest.

The stability of the sapphirine-quartz assemblage has been the source of controversy since Hensen and Green (1973) and Newton (1972) and Newton et al. (1974) published conflicting experimental evidence. In experiments on model pelite compositions at $a(O_2)$ lower than the quartz-fayalite-magnetite buffer, Hensen and Green found that sapphirine-quartz stability was restricted to temperatures in excess of 1030° C at pressures greater than 8 kbars while cordierite-spinel-quartz was restricted to temperatures in excess of 1050°–1150° C at pressures between 2–8 kbars. In contrast Newton (1972) and Newton et al. (1974) synthesized sapphirine-quartz at temperatures as low as 800°–850° C in the $MgO-Al_2O_3-SiO_2$. In the absence of significant experimental progress in the intervening years, this disparity has proved to be a stumbling block in the interpretation of sapphirine-quartz assemblages. However, it is now possible to provide a new insight into this controversy by reference to the distribution of the sapphirine-quartz and related assemblages in the Napier Complex, where temperatures are independently constrained by pigeonite-bearing metasedimentary ironstones (Grew 1982; Sandiford and Powell 1986; Harley 1987). At Fyfe Hills

in Enderby Land, sapphirine-hypersthene-sillimanite-quartz-rutile-ilmenite assemblages require that the P–T conditions were at higher pressure than [spinel, magnetite] in Fig. 7 and between the (garnet) and (cordierite) reactions emanating from this intersection, i.e. at an equivalent temperature but at a higher pressure than this intersection. Meta-ironstones interlayered with these pelites contain textural evidence that pigeonite formed part of a three phase assemblage with augite-orthopyroxene (Sandiford and Powell 1986). The pigeonite composition, $X_{Fe}=0.58$, thereby constrains the metamorphic temperature to have been $1020\pm30°$ C.

The Napier Complex is exposed in oblique profile, with the Fyfe Hills region providing some of the deepest level exposures. In the Tula Mountains, some 100 km east of Fyfe Hills, cordierite-rutile-quartz, sapphirine-rutile-quartz, and sillimanite-hypersthene-rutile-quartz are all found as prograde assemblages (Ellis et al. 1980; Grew 1980; Harley 1985) suggesting P–T conditions were very close to the [spinel, magnetite] intersection in Fig. 7. Ilmenite, with or without rutile, is occasionally present in these pelitic assemblages (Harley 1985). Pigeonite, now inverted, in the Tula Mountains had compositions identical with the Fyfe Hills pigeonite (E.S. Grew, personal communication 1987), confirming the Fyfe Hills constraint that the [spinel, magnetite] intersection is located at temperatures of $1020\pm30°$ C for $a(O_2)$ buffered by, or at lower $a(O_2)$ than, ilmenite-rutile. Geobarometric studies suggest that the Tula Mountains assemblages equilibrated at 7–8 kbars (Grew 1980; Harley 1985), some 2 kbars less than the Fyfe Hills assemblages (Sandiford 1985). Thus, the assemblages associated with sapphirine + quartz-bearing assemblages in the Enderby Land granulites strongly support the experimental results of Hensen and Green. The absence of documented spinel-rutile-quartz assemblages in which spinel is restricted to the system, $FeO-MgO-Al_2O_3-TiO_2-O_2$, provides further support for Hensen and Green's results in as much as it provides circumstantial evidence that this assemblage is restricted to P–T-$a(O_2)$ conditions beyond those of processes affecting pelitic rock compositions.

For magnetite-ilmenite buffered assemblages, the positions of the relevant intersections and appropriate stability fields are not so well constrained. Annersten and Seifert (1981) intersected the (sapphirine, garnet, rutile) univariant under hematite-magnetite buffered conditions in FMASO at 1000° C, suggesting that [garnet, rutile] is located at even higher temperatures. However, the non-appearance of sapphirine in their experimental charges is worrying (Hensen 1986) and may reflect kinetic problems. In natural assemblages from Labwor Hills, prograde cordierite-spinel-magnetite-ilmenite-quartz assemblages coexisted with osumilite and very aluminous hypersthene (11 wt% Al_2O_3) at temperatures greater than [garnet, rutile] (Sandiford et al. 1987). Such alumina contents are comparable with the Napier Complex hypersthenes where osumilite is also known, and suggests prograde equilibration temperatures of at least 1000° C for the Labwor Hills assemblages. Hypersthene produced by reaction across the (sapphirine, garnet, rutile) and (garnet, sillimanite, rutile) reactions contains ~7 wt% Al_2O_3, and this is consistent with temperatures greater than ~900° C for [garnet, rutile] in magnetite-ilmenite-bearing assemblages.

In conclusion, it is clear from our results and those of Hensen that interpretation of reaction textures in sapphirine- and spinel-bearing granulites requires an understanding of the effect of $a(O_2)$ (or Fe_2O_3). Reaction textures cannot be treated as a consequence of P–T vectors unless O_2 is taken into account; they can only be analysed readily if the texture formed in equilibrium with magnetite-ilmenite or ilmenite-rutile. The solution of the outstanding problem posed, but not solved, in this paper, which of Fig. 7a and b is appropriate, should come from study of textures in appropriate high-grade granulites.

Acknowledgement. We would like to thank Bas Hensen for another helpful review.

References

Annersten H, Seifert F (1981) Stability of the assemblage orthopyroxene-sillimanite-quartz in the system $MgO-FeO-Al_2O_3-SiO_2-H_2O$. Contrib Mineral Petrol 77:158–165

Caporuscio FA, Morse SA (1978) Occurrence of sapphirine plus quartz at Peerskill, New York, Am J Sci 278:1334–1342

Droop GTR, Bucher-Nurminen K (1984) Reaction textures and metamorphic evolution of sapphirine-bearing granulites from the Gruf Complex, Italian Central Alps. J Petrol 25:766–803

Ellis DJ, Sheraton JW, England RN, Dallwitz WB (1980) Osumilite-sapphirine-quartz granulites from Enderby Land, Antarctica – mineral assemblages and reactions. Contrib Mineral Petrol 72:353–367

Grew ES (1980) Sapphirine + quartz association from Archaean rocks in Enderby Land, Antarctica. Am Mineral 65:821–836

Grew ES (1982) Osumilite in the sapphirine-quartz terrane of Enderby Land, Antarctica: implications for osumilite petrogenesis in the granulite facies. Am Mineral 67:762–787

Harley SL (1985) Garnet-orthopyroxene-bearing granulites from Enderby Land, Antarctica. Metamorphic pressure-temperature-time evolution of the Archaean Napier Complex. J Petrol 26:818–856

Harley SL (1986) A sapphirine-cordierite-garnet-sillimanite granulite from Enderby Land: implications for FMAS petrogenetic grids in the granulite facies, Antarctica. Contrib Mineral Petrol 94:452–460

Harley SL (1987) A pyroxene-bearing metaironstone and other pyroxene granulites in Enderby Land, Antarctica: further evidence for very high T (>980° C) Archaean regional metamorphism in the Napier Complex. J Metamorph Geol (in press)

Hensen BJ (1986) Theoretical phase relations involving cordierite and garnet revisited: the influence of oxygen fugacity on the stability of sapphirine and spinel in the system $Mg-Fe-Al-Si-O$. Contrib Mineral Petrol 92:363–367

Hensen BJ, Green DH (1973) Experimental study of the stability of cordierite and garnet in pelitic compositions at high pressures and temperatures. III. Synthesis of experimental data and geological applications. Contrib Mineral Petrol 38:151–166

Morse SA, Talley JH (1971) Sapphirine reactions in deep-seated granulites near Wilson Lake, Central Labrador, Canada. Earth Planet Sci Lett 10:325–328

Newton RC (1972) An experimental determination of the high pressure stability limits of cordierite under wet and dry conditions. J Geol 80:398–420

Newton RC, Charlu TV, Kleppa OJ (1974) A calorimetric investigation of the high pressure stability of anhydrous magnesium cordierite with applications to granulite facies metamorphism. Contrib Mineral Petrol 44:25–311

Nixon PH, Reedman AJ, Burns LK (1973) Sapphirine-bearing granulites from Labwor, Uganda. Mineral Mag 39:420–428

Sandiford M (1985) Metamorphic evolution of granulites at Fyfe Hills: implications for Archaean crustal thickness. J Metamorph Geol 3:155–178

Sandiford M, Powell R (1986) Pyroxene exsolution in granulites in granulites from Fyfe Hills, Enderby Land, Antarctica: evi-

dence for 1000° C temperatures in archaean crust. Am Mineral 71:946–954

Sandiford M, Neall F, Powell R (1987) Metamorphic evolution of aluminous granulites from Labwor Hills, Uganda. Contrib Mineral Petrol (in press)

Thompson JB (1979) The Tschermak substitution and reactrons in pelitic schists. In: Zharikov VA, Fonarev VI, Korikovskii SP (eds) Problems in physicochemical petrology (in Russian): Moscow Acad Sci, pp 146–159

Vielzeuf D (1983) The spinel and quartz association in high grade xenoliths from Tallant (S.E. Spain) and their potential use in geothermometry and barometry. Contrib Mineral Petrol 82:301–311

Received May 11, 1987 / Accepted September 29, 1987

Editorial responsibility: Ray Binns